

TIME-AVERAGED BROAD-BAND SPECTRA OF THE DIPPING LOW-MASS X-RAY BINARIES OBSERVED WITH INTEGRAL

S. Balman¹, A. N. Parmar¹, L. Sidoli², A. Paizis², M. Diaz Trigo³, and T. Oosterbroek⁴

¹*Astrophysics Missions Division, Research and Scientific Support Department of ESA, ESTEC, Postbus 299, NL-2200 AG Noordwijk, Netherlands*

²*Istituto di astrofisica Spaziale e Fisica Cosmica-Sezione, di Milano-IASF/INAF, I-20133 Milano, Italy*

³*ESA, ESAC, Urb. Villafranca del Castillo, P.O. Box 50727, 28080 Madrid, Spain*

⁴*Science Payload and Advanced Concepts Office, ESA, ESTEC, Postbus 299, NL-2200 AG, Noordwijk, Netherlands*

ABSTRACT

We present archival data of the dipping LMXB systems, 4U 1916-053, 4U 1323-62, 4U 1624-49, and 4U 1746-37 obtained by the ISGRI and JEM-X detectors on-board the INTEGRAL Observatory. We do not detect a prominent dipping activity in the INTEGRAL energy band of 4.0-200 keV with the exception of 4U 1916-05, however occasional dips in the light curves are recovered. The spectral parameters derived from the fits to the data are consistent with very hot plasma in these systems where the electron temperatures are in a range 4.9-14.6 keV with the exception of 4U 1323-62 having an unbounded temperature with a best fit value of about 300 keV. The optical depth of Compton scattering τ is in a range 2.1-0.004. We interpret that the dipping LMXBs presented in this work host hot extended large coronal structures. We suggest that the INTEGRAL data of 4U 1323-62 reveals no cut-off energy.

Key words: X-ray binaries – Accretion, accretion disks – X-rays:individual: 4U 1323-620, 4U 1916-053, 4U 1624-490, 4U 1746-371.

1. INTRODUCTION

Around 10 galactic low-mass X-ray binaries (LMXBs) exhibit periodic dips in their X-ray intensity. The dips recur at the orbital period of the system and are believed to be caused by periodic obscuration of a central X-ray source by structure located in the outer disk resulting from the impact of the accretion flow from the companion star into the disk [25]. The depth, duration and spectral properties of the dips change according to the source and with cycle. The spectral changes during LMXB dips are complex and cannot be well described by a simple increase in column density of cold absorbing material with normal abundances [19], [8], [21].

Modeling of these spectral changes provides a powerful

probe of the structure and location of the emitting and absorbing regions in LMXBs [6], [7], [10]. In the *complex continuum* approach, the X-ray emission is assumed to originate from a point-like blackbody, or disk-blackbody component, together with an extended power-law component. This approach primarily models the spectral changes during dipping intervals by the partial and progressive covering of the power-law emission from an extended source which is an ADC (accretion disk corona). The absorption of the point-like component is allowed to vary independently from that of the extended component, and usually no partial covering is included. The power-law emission component can be modeled by a generic power-law model with a cut-off energy in accordance with the energy of the scattering electron population. More physically realistic models involve the geometry, the incident photon temperature into the Comptonizing region, the scattering characteristics of the Comptonizing electrons like the mean number of scatterings and relativistic effects [22], [11].

The improved sensitivity and spectral resolution of *Chandra* and XMM-Newton is allowing narrow absorption features from highly ionized Fe and other metals to be studied from a growing number of X-ray binaries. These features were first detected from micro-quasars [24], [14]. More recent *Chandra* High-Energy Transmission Grating Spectrometer (HETGS) observations of the black hole candidate GX 339-4 [16] revealed the presence of blue-shifted and absorption features indicative of a highly-ionized outflow. The LMXB systems that exhibit narrow X-ray absorption features are all known dipping sources (see Table 5 of [4]) except for GX+13 which shows deep blue-shifted Fe absorption features in its HETGS spectrum, indicative of out flowing material [23]. The lack of any obvious orbital phase dependence of the LMXB absorption features (except during dips), suggests that the absorbing plasma is located in a cylindrical geometry centered on the compact object. Moreover, new *Chandra* findings reveal that the warm absorbing plasma is not in photoionization equilibrium and that there is rather a distribution of different ionization across the absorbing medium (e.g., [12]).

Table 1. LMXBs Properties. L_{36} is the 0.6–10 keV unabsorbed luminosity in units of 10^{36} erg s^{-1} . (see Diaz Trigo et al. 2006).

LMXB	P_{orb} (hr)	L_{36} (erg s^{-1})	d (kpc)	Dips/ Eclipses
4U 1916-053	0.83	4.4	9.3	D
4U 1323-62	2.94	5.2	10	D
4U 1746-37	5.16	10.1	10.7	D
4U 1624-49	20.88	47.5	15	D

2. DATA AND OBSERVATIONS

The INTEGRAL observatory consists of two gamma-ray instruments, one optimized for 15 keV to 10 MeV high-resolution imaging (IBIS) and the other for 20 keV to 8 MeV high-resolution spectroscopy (SPI) [26]. The extremely broad energy range of IBIS is covered by two separate detector arrays, ISGRI (15–500 keV) and PICsIT (0.2–10 MeV). The payload is completed by X-ray (JEM-X; [15]) and optical monitors (OMC; [16]).

The data used here were obtained from the public archive at the INTEGRAL Science Data Center (ISDC; [9]). Public data from revolutions 30 to 250 (2002 to 2004) were used. The data were processed using the Off-line Scientific Analysis (OSA 5.1) software provided by the INTEGRAL Science Data Center. After the standard data pipeline processing (dead time correction, good time-interval selection, gain correction, energy reconstruction), the source spectra and background subtracted light curves were derived using the general prescriptions indicated by OSA 5.1. The source positions were fixed in order to derive correct fluxes for the sources. For further data manipulation, we used standard analysis softwares like FTOOLS 6.0.4 and XSPEC 12.2.1. Table 1 lists the characteristics of the LMXBs studied in this paper.

The 4.0–200.0 keV light curve derived for the four LMXBs do not show a very prominent dipping activity. On the other hand, we were able to recover the dipping activity in this energy range, by folding the light curve with the well known orbital period. Figure 1 below shows the light curve of 4U 1916-05 folded with the ephemerides in [5]. The modulation of the JEM-X light curve is about 18% peak-to-peak in the 3–10 keV energy band (% peak-to-peak $\sim (\text{max rate} - \text{min rate})/(\text{max rate} + \text{min rate})/2$). For the other sources, we do not recover very prominent dipping activity because of the large associated error in the orbital period or that the source is generally dim. For example, 4U 1624-49 shows more of a flaring light curve than the large scale dips that are recovered from this source [2].

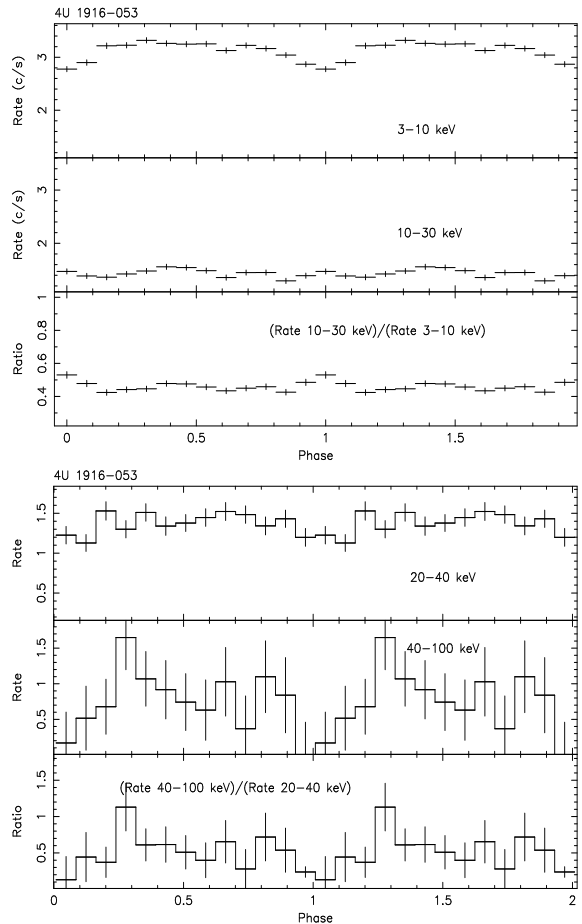


Figure 1: The JEM-X light curve of the 4U 1916-053 (bin time is 10 sec) top panel and the bottom panel shows the folded ISGRI light curve (bin time is 120 sec). The orbital period is 3000.6508 sec (used ephemerides in [12]).

3. THE BROAD-BAND LMXB SPECTRA

We performed spectral analysis using XSPEC version 12.2.1 [1]. We used the photo-electric cross sections of [18] to account for absorption by the neutral gas with solar abundances (wabs model in XSPEC). Spectral uncertainties are given at 90% confidence level ($\Delta\chi^2 = 2.71$) and upper limits at 95% confidence. We regrouped the ISGRI and JEM-X spectra to increase signal to noise in the energy bins. To account for systematic effects we added quadratically a 1% uncertainty to each spectral bin.

We fitted the data with several composite models including neutral hydrogen absorption, a disk black body or a black body emission and a cutoff power-law or COMPTT [22] model of emission. Constant factors were included in the spectral fitting to allow for normalization uncertainties between the JEM-X and ISGRI instruments. These factors were constrained to be within their usual ranges in the spectral analysis. During the fitting procedure we kept the values of the neutral hydrogen absorption fixed at the values derived from the XMM data except for 4U 1624-49 [10]. We also applied a single model

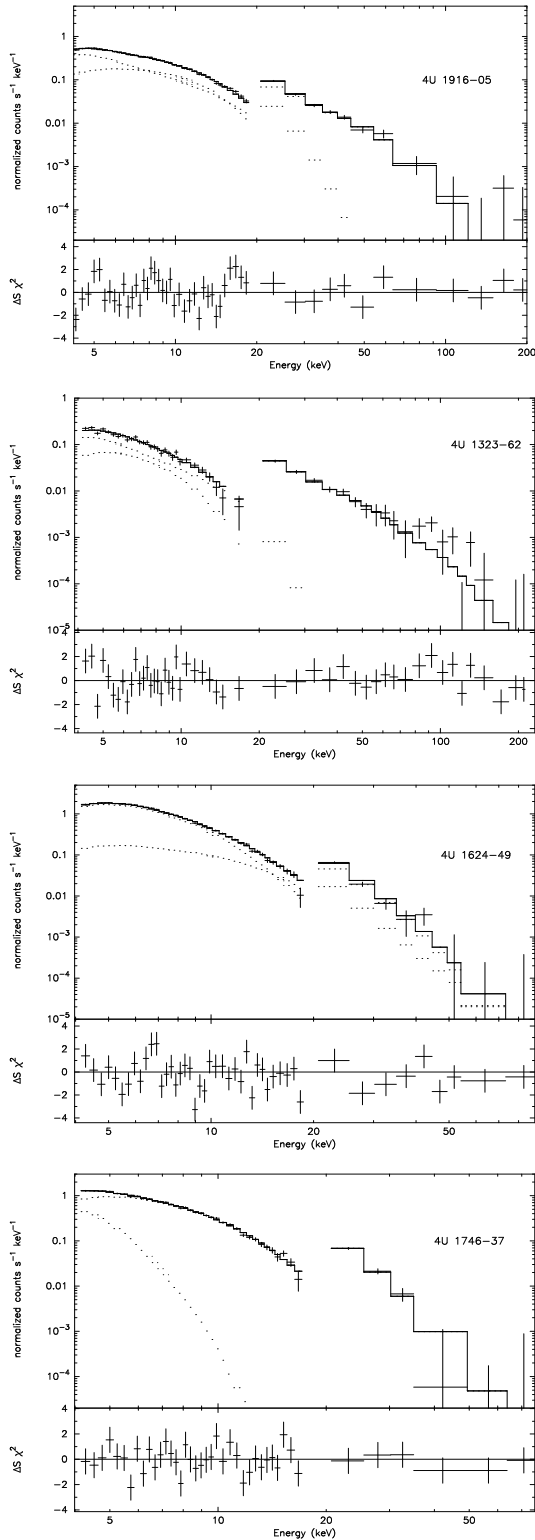


Figure 2: The simultaneously fitted JEM-X and ISGRI spectra of the four dipping LMXBs in the 4-200 keV energy range (4-20 keV: JEM-X and 20-200 keV: ISGRI). The spectra displayed from top to bottom panels are of 4U 1916-053, 4U 1323-62, 4U 1624-49 and 4U 1746-37, respectively. The crosses indicate the data, and the solid and dashed lines show the fitted models. The second panel under each spectra display the residuals in sigmas.

of cut-off power law or COMPTT to fit the four broadband spectra and we do not find any consistent fit with $\chi_{red}^2 < 2.5$ except for 4U 1323-62. Figure 2 shows the fitted broad band spectra using JEM-X and ISGRI data.

4. DISCUSSION

We presented the JEM-X and ISGRI spectra of the four sources 4U 1916-05, 4U 1323-62, 4U 1624-49 and 4U 1746-37. The spectra is equivalent to the persistent emission from these sources averaged over time. This is a unique test that could be done with the INTEGRAL observatory. During the time span of our data, we do not detect a prominent high or low state of any of the LMXBs in our sample. INTEGRAL results yield for the first time the plasma temperature of the Comptonizing regions in these systems together with the Compton optical depths revealing the accretion geometry and the location of ionized absorbers in these systems.

In general, the X-ray flux and luminosity between 4.0-200.0 keV for individual sources are larger by a factor of 1.3-2 compared with the previous findings between 0.6-10 keV except for 4U 1323-62 which is about a factor of 2 less compared with [4]. The individual values are in a range $2.2-58.8 \times 10^{36} \text{ erg s}^{-1} \text{ cm}^{-1}$. Results with the the Cut-off power law model show that the time average data yield different parameters for $E_{cut-off}$ and the photon index. For 4U 1916-05, [7] find $\Gamma=1.87$ and $E_c=80$ keV where we have almost a similar photon index but a different cut-off energy $E_c=20.4$. For 4U 1624-49, [2] find $\Gamma=2.0$ and $E_c=12$ keV where we find an inconsistently negative photon index and very low $E_c < 5.0$ keV (including error ranges). Most likely this is not a correct model for the spectrum of 4U 1624-49. For 4U 1746-37, [20] find $\Gamma=0.39$ and $E_c=3.5$ keV where we find $\Gamma=2.18$ and $E_c=6.74$ keV. For 4U 1323-62, [3] find $\Gamma=1.96$ and $E_c=44$ keV where we find $\Gamma=3.0$ and an unbound cut-off energy. We also note that the previous results are not in the 90% confidence level error ranges, we derive for the four dipping LMXBs. We find a range of temperatures from 4.9-14.56 keV (best fit results) for the plasma temperature in the Comptonizing regions using the COMPTT model in XSPEC. The plasma temperature of 4U 1323-62 is about 300 keV and the parameter is unconstrained. The optical depth of Compton scattering τ is in a range 2.1-0.004 which shows that the Comptonizing regions are tenuous.

ACKNOWLEDGMENTS

Based on observations with INTEGRAL, an ESA project with instruments and science data centre funded by ESA member states (especially the PI countries: Denmark, France, Germany, Italy, Switzerland, Spain), Czech Republic and Poland and with the participation of Russia and the USA. SB acknowledges an ESA fellowship and

also TUBA-GEBIP scholarship from Turkish Academy of Sciences.

REFERENCES

- [1] Arnaud, K.A., in ASP Conf. Ser. 101: Astronomical Data Analysis Software and Systems V, 17, 1996.
- [2] Balucinska-Church M., Humphrey P.J., Church M. and Parmar A.N., *A&A* 360, 583, 2000.
- [3] Balucinska-Church M., Church M., Oosterbroek T. et al., *A&A* 349, 495, 1999.
- [4] Boirin L., Mendez M., Diaz Trigo M., Parmar A.N. and Kaastra J.S., *A&A* 436, 195, 2005.
- [5] Chou Y., Grindlay J.E., and Bloser P.F., *ApJ* 549, 1135, 2001.
- [6] Church M.J., and Balucinska-Church M., *A&A* 300, 441, 1995.
- [7] Church M.J., Parmar A.N., Balucinska-Church M., et al., *A&A* 338, 556, 1998.
- [8] Courvoisier T.J.L., Parmar A.N., Peacock A., and Pakull M., *ApJ* 309, 265, 1986.
- [9] Courvoisier, T.J.L., Walter, R., Beckmann, V. et al., *A&A*, 411, L53, 2003.
- [10] Diaz Trigo M., Parmar A. N., Boirin L., Mendez M. and Kaastra J.S., *A&A* 445, 179, 2006.
- [11] Hua X-M. and Titarchuk L., *ApJ* 449, 188, 1995.
- [12] Juett A.M. & Chakrabarty D., *ApJ* 646, 493, 2006.
- [13] Kotani T., Ebisawa K., Dotani T. et al., *ApJ* 539, 413, 2000.
- [14] Lee J.C., Reynolds C.S., Remillard R. et al. 2002, *ApJ* 567, 1102, 2002.
- [15] Lund N., Budtz-Jorgensen C., Westergaard N. J. et al., *A&A* 411, 231, 2003.
- [16] Mas-Hesse J.M., Gimenez A., Culhane J.L. et al., *A&A* 411, L261, 2003.
- [17] Miller J.M., Raymond J., Fabian A.C. et al., *ApJ* 601, 450, 2004.
- [18] Morrison R. and McCammon D., *ApJ* 270, 119, 1983.
- [19] Parmar A.N., White N.E., Giommi P. and Gottwald M., *ApJ* 308, 199, 1986
- [20] Parmar A.N., Oosterbroek T., Guainazzi M. et al., *A&A* 351, 225, 1999.
- [21] Smale A., Mukai K., Williams R., Jones M.H. and Corbet R., *ApJ* 400, 330, 1992.
- [22] Titarchuk L., *ApJ* 434, 570, 1994.
- [23] Ueda Y., Mukarami H., Yamaoka K., Dotani T. and Ebisawa K., *ApJ* 609, 325, 2004
- [24] Yamaoka K., Ueda Y., Inoue H., *PASJ* 53, 179, 2001.
- [25] White N.E. and Swank J. H., *ApJ* 253, L61, 1982.
- [26] Winkler C., Courvoisier T. J., Di Cocco G. et al., *A&A* 411, L1, 2003.